COMPOSITES & POLYCON 2009
American Composites Manufacturers Association
January 15-17, 2009
Tampa, FL USA

Behavior of Natural-Fiber/Thermoplastic Sheet Piling

Daniel Alvarez-Valencia, Habib J. Dagher, Roberto A. Lopez-Anido, William G. Davids, Douglas J. Gardner
AEWC Composites Center, University of Maine.

Abstract

This paper describes the flexural behavior of an innovative Natural-Fiber/Thermoplastic Composite (NFTC) also known as Wood Plastic Composite (WPC) sheet piling. Test methods were developed and full-scale bending tests were conducted to characterize the flexural performance of the piles as part of a larger effort to develop a structural design methodology. In this study, WPC sheet piling specimens were produced at the Advanced Engineered Wood Composites (AEWC) Center at the University of Maine. Tensile coupon tests were performed to identify material properties. Full scale four-point bending tests were conducted up to failure on 20 sets of joined pairs of Z-piles of four different span lengths. Following the static tests, cyclic loading with amplitude equal to 40% the mean ultimate strength was performed to assess residual deformation under repeated loading. Data analysis includes moment capacity, modulus of rupture, apparent modulus of elasticity, and failure modes. Test results indicate that the structural test method is adequate for WPC sheet piling and assures its reproducibility. Compression failures or buckling of the compression flanges were not observed, and the C-T joints did not restrict the rotation of joined piles with respect to one another. Specimens show a linear load-deflection behavior up to 40% of the ultimate strength. Short spans failed predominantly in shear while longer spans failed in flexural tension. Specimens fail without significant yielding, and the ultimate strength is reached at failure. The findings show significant promise for Natural-Fiber/Thermoplastic light duty sheet piling retaining wall structures.

Introduction

Wood Plastic Composites (WPC) have primarily been used for non-structural applications. For several decades the WPC industry has expanded and established itself in markets that include the automotive, building and furniture industries [1]. The continuous growth of WPC and advantages including moisture resistance and low maintenance [2] have led to research into WPC waterfront structural applications [3]. At the University of Maine AEWC Composites center, reinforced built-up WPC sections [3] and WPC box beam sections have been developed in an effort to find alternative wood-based structural composites.

This study is part of an investigation, into the structural use of extruded WPCs for transportation applications. Retaining wall structures like that shown in Figure 1 are used in waterfronts, fills and excavations. Conventional materials used in these applications include pressure-treated wood, vinyl, reinforced concrete and steel. Several durability concerns exist with these materials, including fungal attack and biodegradation of wood [3], and rapid corrosion of steel and reinforced concrete systems [4]. In addition chemically treated wood is subject to strict environmental regulations. These concerns increase life-cycle cost [5], making WPC an attractive alternative for waterfront structures.

Previous structural optimization studies at the University of Maine [6] developed a voided flange and web Z-section sheet piling, suitable for a WPC retaining wall system. Considering the capacity of the extruder at the AEWC Center, a 254mm (10in) deep Z-shape voided WPC section was designed and produced in the laboratory.

Little literature is available on sheet piling structural systems using non-conventional materials. However, non-conventional materials like FRP and PVC sheet pilings systems have been developed and their flexural properties have been studied considering ASTM D 790 ([4], [7], [8]). ASTM D 7031 [9] is the standard guide for evaluating mechanical and physical properties of WPC products. Section 5.5 of this standard addresses bending and references test methods D 4761 [10] or D 6109 [11] as the principles to follow for testing.

The objective of this paper is to characterize the flexural behavior of an extruded hollow cross section WPC sheet piling as part of a larger effort to develop a structural design methodology. Considering that there are no established test methods for WPC sheet pilings, testing fixtures were developed and testing procedures modified. These test methods were based on ASTM D 7031 [9], D 4761 [10], D 6109 [11], D 198 [12], D 790 [13] and D 6272 [14].

Experimental Work

Material

The WPC Z-shape hollow cross section sheet piling was produced at the AEWC center at the University of Maine, using a Davis Standard Woodtruder™ with a gravimetric feeding system (Figure 2-a). This WPC is composed of 50% wood flour by weight (Figure 2-b), polypropylene (Figure 2-c), and additives. The formulation consists of pine wood flour provided by American Wood Fiber, an enhanced polypropylene resin provided by BP Amoco, commercial lubricant package, ultraviolet light stabilizer with polyethylene colorant base, and a coupling agent. The extruder conveys the WPC material through the temperature controlled die as shown in Figure 3. One of the challenges includes proper cooling to maintain the cross-sectional shape. In this case, after the final product exits the die, no cooling process was provided; ambient temperature and extruding speed gave enough time for the extrudate to solidify maintaining the cross-sectional shape (Figure 4).

Material Properties

Tensile tests were employed to characterize the material properties. Testing followed ASTM D 638 [15]. Coupons were cut from the extruded sheet pilings, and machined to comply with type III specimens showed in the sketch in Figure 5 [15]. Coupon type was selected considering that the material's available thickness was between 7 to 14 mm (0.28 to 0.55 in).

Tests were performed with a 100 kN (22 kip) Instron servo hydraulic floor model dynamic system. Load, displacement, and extensometer readings were monitored and recorded during testing (see Figure 6). Eight WPC specimens were tested in tension up to failure at a constant nominal strain rate of 1 % per minute. Following ASTM D638, conditioning and testing was carried out at a temperature of 23 ± 2ºC (73.4 ± 3.6ºF), and relative humidity of 50 ± 5%.

Results and Discussion

Material Properties

Figure 7 shows the stress-strain curve for all the specimens tested and the mean apparent modulus of elasticity (MOE). WPC exhibits an initial linear stress-strain response followed by a nonlinear behavior up to failure. Using a linear regression analysis it was observed that all specimens show a linear elastic behavior up to approximately 40% of the ultimate strength. This verifies the validity of calculating the MOE using a linear regression between 10 and 40% of the ultimate strength as per ASTM D 7031 for WPC. Specimens fail in tension along the narrow section, with an irregular surface across the specimen (Figure 8).

Mean values and coefficient of variation (COV) for MOE, ultimate strength, strain at ultimate strength, maximum strain, and strength at maximum strain are shown in Table 1. The mean MOE mean value is 3.00 GPa (435 ksi) and the mean ultimate strength (UTS) is 12.7 MPa (1.84 ksi). Variability was low compared to wood with COVs below 7%. Strain at ultimate strength and maximum strain approach the same value of 1%, and both quantities have approximately the same COV of 15%. The mean strength at failure is lower than the mean ultimate tensile strength, which may indicate that necking occurred. Based on this observation, three regions of the stress-strain curve are defined as shown in Figure 7: elastic region (constant MOE), plastic region, and necking region.

WPC has higher stiffness than some thermoplastics. Table 2 gives the MOE values for WPC and a variety of polymers. Design of members for structural applications often considers the materials to be subject to stresses within the linear range, and deflections may limit member capacity. WPC's increased stiffness relative to that of many pure polymers is promising. It should be noted that future WPC material level-testing should address other important factors such as moisture effects, freeze-thaw durability, creep deformations and creep rupture.

Structural Testing Program

To characterize the flexural behavior of the WPC sheet pilings, four-point bending tests based on ASTM standards ([9], [10], [11]) were conducted at the AEWC Center at the University of Maine. The specimens tested were twenty sets of joined pairs of Z-piles with span lengths of 2.7 m (9 ft), 3.9 m (13 ft), 4.7 m (15.5 ft) and 5.9 m (19.5 ft) were tested (see Table 3). The configuration selected resembles the installed sheet piling under regular loading.

Test Method

Tests were performed with a 244 kN (55 kip) Instron hydraulic actuator. A steel wide-flange beam was utilized as a spreader, and two load heads were attached to it. Two reinforced concrete barriers were the external supports of the test set-up (Figure 9). Simulating service conditions, the sheet pilings were restricted from lateral movement and rotation at the four points of contact (2 supports, and 2 points of load application). Steel braces were designed for this purpose following the joined paired sheet piling cross-section (Figure 9). Neoprene pads were placed along the brace points of contact with the piles. To constrain the piles, straps were installed along the length [18], spaced at 0.61 m (2 ft) (see Figure 10). Tests were conducted at 1 % per minute extreme fiber strain rate up to specimen failure.

Following the quasi-static tests, cyclic loading reaching 40% of the mean ultimate strength for 100 cycles was performed on one specimen of each span length to assess residual deformation under repeated loading.

Two different methods were used to record deflections under testing. Both methods recorded deflections at mid span, along the top and bottom flanges. The first method consisted of string potentiometers (cable-extension transducers [19]) attached to the sheet pilings at the locations shown in Figure 10. The second method involved the *PONTOS* non-contact optical 3D measuring system (see Figure 11) [20]. Based on the use of digital images, this system records and processes object deformations, movements, and dynamic behavior of unlimited locations in one or multiple objects. It is composed of a set of digital cameras that can be installed in any location and orientation and must be calibrated to analyze the specific 3D volume needed. Targets and reference points must be installed; the software's main function consists of finding ellipses (points) in the images to assign coordinates to the pixels. Step by step deflections can be observed, specific calculations can be programmed, tables of results can be exported and visual aids such as movies and snapshots make it a useful and versatile system. In this case, the use of the optical system also prevented the damage of conventional measuring equipment (string potentiometers, linear variable displacement transducers LVDT) in the events of abrupt failures.

Results and Discussion

Quasi-Static Bending

Failure modes

The WPC sheet pilings tested in four-point bending failed in either shear or tension, depending on the span. The 5.9 m (19.5 ft) long sheet pilings failed in bending, whereas the shorter piles with a 2.7 m (9 ft) span failed predominantly in shear. As expected, bending failure occurred within the middle third region of the beam, in which the bottom flange failed in tension (see Figure 12). The shear failures initiated within the outside thirds of the sheet pilings near the load application points, and were characterized by a near 45 degree crack that formed in the web area (Figure 13). Whether shear or bending, failure was always located in one of the two adjoining piles, but both adjoining piles never failed simultaneously. Some cracking however was observed to propagate slightly into the adjacent (intact) sheet piling's top flange. In some cases for the intermediate spans (3.9 m (13 ft), 4.1 m (15.5 ft)), it was difficult to identify a shear or bending failure, particularly since both types of failures were commonly observed near the load application points.

Compression failures or buckling of the compression flanges were not observed. This demonstrates that the voided structures provided enough stability for the section to prevent premature compression buckling failures.

Cross-section behavior

A typical four-point bending deflection displacement field for a 5.9 m (19.5 ft) sheet piling is shown in Figure 14. A single curvature takes place along the top flanges during testing for the entire spans analyzed; buckling of the compression flanges was not present. Braces and straps constrain the sheet pilings, simulating the effect of the installed sheet pilings. Even though these are present, the cross-section displacement field at mid-span indicates that distortions are taking place while testing. The distorted shape under load is sketched in Figure 15a, and measured cross-section displacement field in Figure 15b shows the typical maximum deflections for a 5.9 m (19.5 ft) sheet piling at various points on the cross-section at mid-span.

Deflection along the cross-section follows a particular path during testing. Figure 16 shows the difference in deflection between the bottom flange minus the deflection of the top flange, plotted against load. One specimen per span is shown in the figure. The process starts with higher deflection values at the bottom flange followed by the rotations shown in Figure 15a resulting in higher top flange deflections. As the span increases, the distortion of the section increases in both the initial and final stages of the test. It is observed that the C-T joints do not restrict the rotation of joined piles with respect to one another.

Load-deflection curves

Actuator applied load vs. sheet piling web deflection at mid span for the different span lengths tested are shown in Figure 17. Following the behavior of WPC, elastic and plastic regions can be appreciated in the load-deflection curves. Using a linear regression analysis, it was observed that all specimens show a linear elastic behavior up to 40% of the ultimate strength. This verifies the validity of calculating the MOE using a linear regression between 10 to 40 % of the ultimate strength per ASTM D 7031. During the plastic region (non-linear), the slope of the load-deflection curve diminishes resulting in higher deflections with the same increment of loadings. Specimens fail without yielding; consequently, the ultimate strength takes place at failure.

Flexural properties

Cross-sectional dimensions were measured for a number of specimens. An average moment of inertia of 2.2E-4 m^4 (0.0256 ft^4) and neutral axis of 0.129 m (0.424 ft) was found for the joined pair Z-shape sheet piling configuration. Performance measures include apparent flexural modulus of elasticity (E), modulus of rupture (MOR), and deflection at failure.

The apparent elastic modulus E was calculated assuming a linear elastic behavior between 10 to 40 % of the mean ultimate strength [9]. Using a linear regression analysis, the value of load over deflection (P/Δ) was found for each test. Assuming a homogenous and linear elastic simple beam with two equal concentrated loads symmetrically placed, and the beam relations [21] given below, the apparent E (equation [1]) and modulus of rupture (MOR) (equation [2]) were found.

$$E = \frac{P/2 \cdot l^3}{28 \cdot \Delta \cdot I} \qquad [1]$$

$$S_R = MOR = \frac{P \cdot l}{6} \cdot \frac{c}{I} \qquad [2]$$

Where:
E = Apparent flexural modulus of elasticity,
P = load,
l = beam length,
Δ = beam deflection,
I = moment of inertia,
c = distance from neutral axis to extreme tension fiber, and
MOR = modulus of rupture.

Mean apparent flexural modulus of elasticity (E) is 6.05 GPa (878 ksi) with a COV of 9%. Table 4 shows how the value fluctuates between the different spans analyzed, indicating a general range of approximately 5 to 6.5 GPa (725 to 942 ksi). The variation of 9 % between the different spans indicates the homogeneity of the WPC sheet pilings and reproducibility of the test method.

Testing methods followed recommend a span-to-depth ratio of no less than 16 ([9], [10], [11], [13], [14]). With the WPC sheet piling geometry, bending tests should be done on spans higher than 3.9 m (13 ft). The shorter spans (2.7 m (9 ft)) have a span/depth ratio of 10.8, they present the highest data variation (COV = 20%) and mean MOR value of 11.9MPa (1.73 ksi). Comparing this MOR value with the mean ultimate tensile strength of the WPC of 12.7 MPa (1.84 ksi), indicates that the material failed predominantly in shear. MOR values for the spans with span-to-depth ratio higher than 16 (3.9 m (13 ft), 4.7 m (15.5 ft), and 5.9 m (19.5 ft)) were higher than the mean ultimate tensile strength, indicating tension failure (see Table 4). As the span shortens shear stresses increase; consequently, the WPC sheet piling strength and geometry is not used to its bending capacity. Mean MOR for the different spans are shown in Figure 18.

Flexural stiffness *EI* is a performance level used for sheet piling systems. The WPC mean EI is 1.38E6 N-m^2/m (1.47E5 kip-in^2/ft). This value lies below the light duty sheet piling category [22], and above the very light duty sheet-piling group [23]. As expected, deflection increases with increasing span, Table 4 values show a maximum of 0.036 m (0.117 ft) being approximately 1% the beam length for the 2.7 m (9 ft) span and 0.219 m (0.72 ft), being approximately 4% the beam length for the 5.9 m (19.5 ft) span.

Cyclic Bending

Following the quasi-static tests, for 1 specimen per span, cyclic loading reaching 40% of the mean ultimate strength for 100 cycles was performed at 1 % per minute extreme fiber strain rate. Residual deformation under repeated loading is given in Table 5. Figure 19 shows a typical load-deflection curve. Constant rigidity of the beam during the loading sequence is observed. The WPC sheet pilings are not truly linearly elastic under cyclic loading, and small permanent deformations accumulate. This is a topic warranting further study to quantify its significance in structural applications.

Summary and Conclusions

This study of the flexural behavior of WPC sheet pilings has addressed basic material properties and their performance in bending.

Tensile coupon test specimens exhibit a linear stress-strain behavior up to 40% of the ultimate strength. This justifies the calculation of the MOE using a linear regression between 10 to 40 % of the ultimate strength per ASTM D 7031.

Four-point bending test results indicate that the test configuration used in this study gives repeatable results and reasonable failure modes. Short spans failed predominantly in shear while longer spans in tension. The ultimate strength coincides with failure.

Compression failures or buckling of the compression flanges were not observed, demonstrating the stability of the voided Z-section used in this study. The inter-pile C-T joints did not restrict the rotation of adjacent piles with respect to one another.

Cyclic flexural tests conducted in the linear load-deflection range indicate that small permanent deformations do accumulate, although there is no apparent stiffness degradation.

Ongoing and future work includes creep testing, which is expected to quantify pile response under sustained loads. In addition, durability testing will be conducted to examine the effects of moisture, freeze-thaw cycling and UV exposure on WPC material properties. Ultimately, design tables will be developed to allow the rapid specification of WPC sheet pilings for a range of soil types and wall heights.

Acknowledgements

This work is an ongoing research project on the transportation applications of WPC, sponsored by the Federal Highway Administration, FHWA contract #DTFH61-06-C-0064 and conducted at the University of Maine - Advanced Engineered Wood Composites (AEWC) Center.

Authors

Daniel Alvarez-Valencia: Mr. Alvarez-Valencia is a M.S. Student at the University of Maine. His thesis research is related to WPC sheet piling systems.

Habib J. Dagher: Dr. Dagher is a Professor of Civil/Structural Engineering at the University of Maine. He is the Director of the AEWC Composites center at the University.

Roberto A. Lopez-Anido: Dr. Lopez-Anido is an Associate Professor in the Department of Civil and Environmental Engineering at the University of Maine. His research areas focus on mechanics and durability of composite materials.

William G. Davids: Dr. Davids is an Associate Professor of Civil/Structural Engineering at the University of Maine. His research areas focus on structural mechanics, analysis and design.

Douglas J. Gardner: Dr. Gardner is a Professor of Wood Science & Technology at the University of Maine. His research areas focus on polymer science and surface chemistry.

References:

[1] C. Clemons. Forest Products Journal. 52 [6]. 10 (2002).

[2] W. Chetanachan, Journal of vinyl and additive technology 7 [3], 134 (2001).

[3] H. J. Dagher, M. A. Iqbal, R. Lindyberg, D. Gardner and W. Davids. "Project end report, Naval Advanced Wood Composites, Materials and Section Mechanics", October 2003.

[4] U. K. Vaidya, A. A. Villalobos and J. C. Serrano-Perez, Proceedings of the International Offshore and Polar Engineering Conference, Seul, Korea, 454 (2005).

[5] D. F. MacGraw and P. M. Smith, Forest Product Journal, 57 [3], 76 (2007).

[6] M. J. Kahl. "Structural design of hollow extruded WPC sheet piling," Master's thesis, The University of Maine, Department of Civil and Environmental Engineering, 2005, pp. 1,146.

[7] C. Giroux and Y. Shao. Journal of Composites for Construction, 7 [3], 348-355 (2003).

[8] Y. Shao, Journal of Materials in Civil Engineering 18 [5], 626-633 (2006).

[9] ASTM D 7031-04 Standard Guide for Evaluating Mechanical and Physical Properties of Wood Plastic Composite Products. 2004.

[10] ASTM D 4761-05 Standard Test Methods for Mechanical Properties of Lumber and Wood-base Structural Material. 523-532. 2005.

[11] ASTM D 6109-05 Standard Test Methods for Flexural Properties of Unreinforced and Reinforced Plastic Lumber and Related Products. 2005.

[12] ASTM D 198-05a Standard Test Methods of Static Tests of Lumber in Structural Sizes. 2005.

[13] ASTM D 790-03 Standard Test Methods for Flexural Properties of Unreinforced and Reinforced Plastics and Electrical Insulating Materials. 1-11. 2003.

[14] ASTM D 6272-02 Standard Test Methods for Flexural Properties of Unreinforced and Reinforced Plastics and Electrical Insulating Materials by Four-Point Bending. 2002.

[15] ASTM D 638-03 Standard Test Methods for Tensile Properties of Plastics. 47-60. 2003.

[16] R. J. Fried, Polymer Science and Technology. Prentice Hall PTR, 2003, pp. 194.

[17] IEEE/ASTM SI 10-2002 American Standard for use of the International System of Units (SI): The Modern Metric System. 1. 2002.

[18] L. Ellen Lackey, J. G.Vaughan and W. Wimbrow, Proceedings ACMA's Composites and Polycon, Tampa, FL USA. October (2007).

[19] Celesco Transducer Products, Inc. String Pots. http://www.celesco.com, Accessed 7-17-2008.

[20] GOM mbh, "Pontos v6 User Manual – Software", Germany, 2007.

[21] American Institute of Steel Construction INC, Steel Construction Manual, (2005).

[22] P. K. Dutta and U. Vaidya, "A Study of the Long Term Application of Vinyl Sheet Piles," US Army Corps of Engineers, August 2003.

[23] R. Lampo, T. Nosker, P. Dutta and R. Odello. Proceedings of the 1998 Ports Conference. Part 2 (of 2), Long Beach, CA, USA. Mar 1998, pp. 830,839.

Figures:

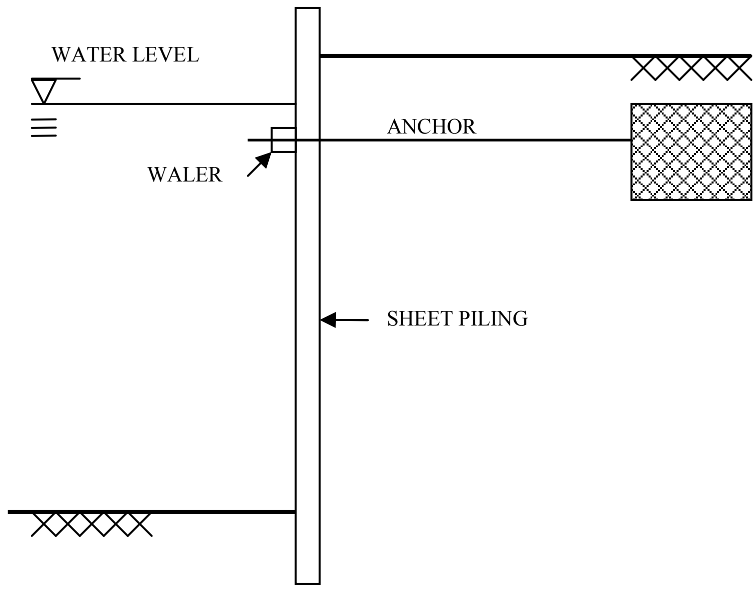

Figure 1. Sheet Piling Application

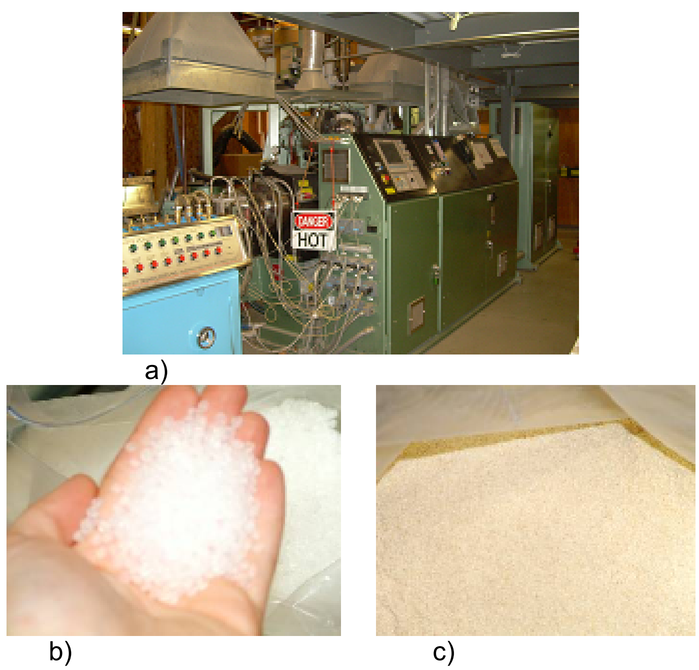

Figure 2. Equipment and Materials a) Extruder, b) Polypropylene Pellets, c) Wood Flour

Figure 3. WPC Z-Section Extrusion Die

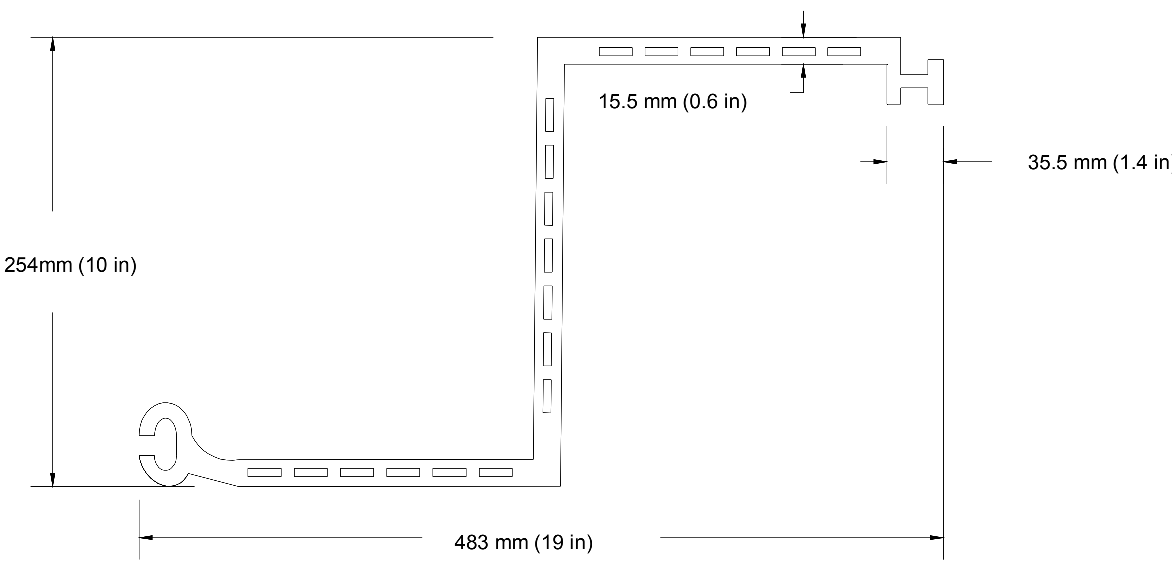

Figure 4. Cross-Section of the WPC Sheet Piling

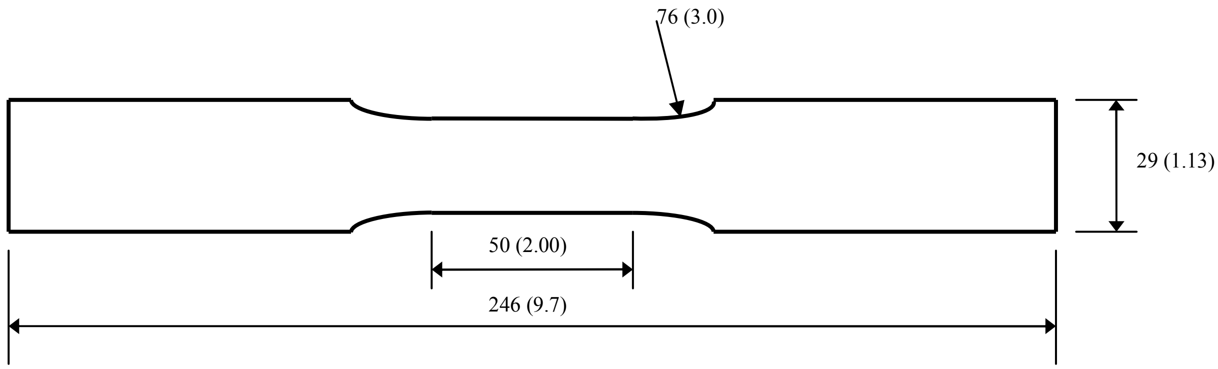

Figure 5. Tensile Coupon Type III, per ASTM D-638. Not to scale. mm (in)

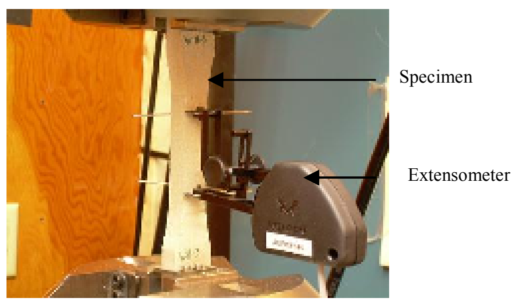

Figure 6. Tensile Test set-up.

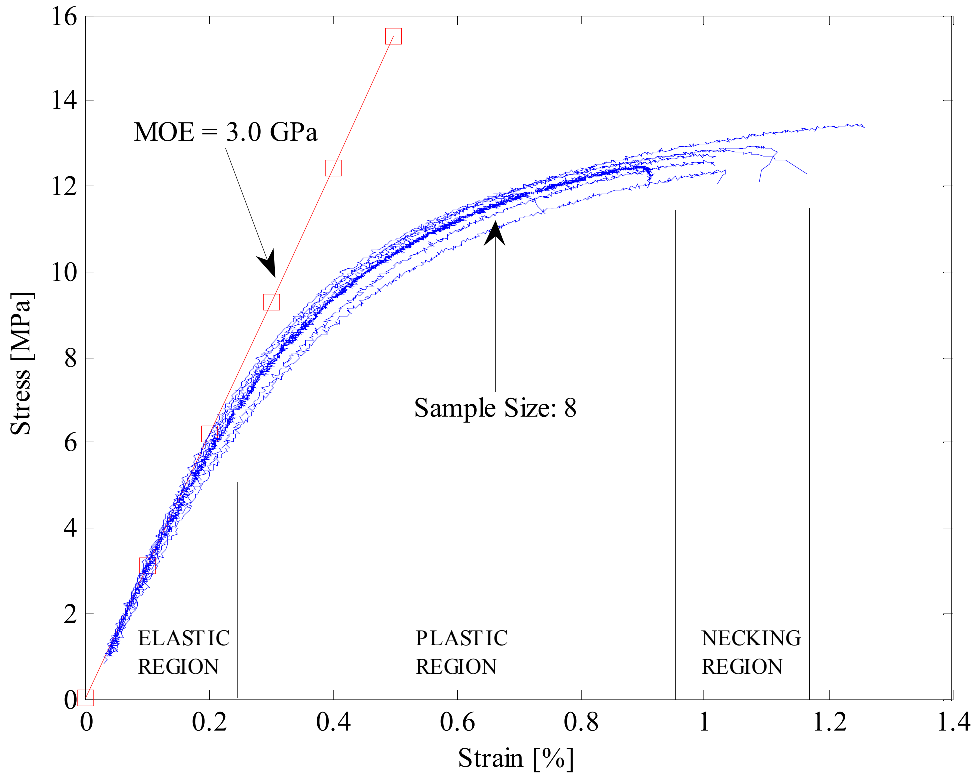

Figure 7. Stress-Strain Curve for WPC. 8 Specimens Tested at 1% Nominal Strain Rate.

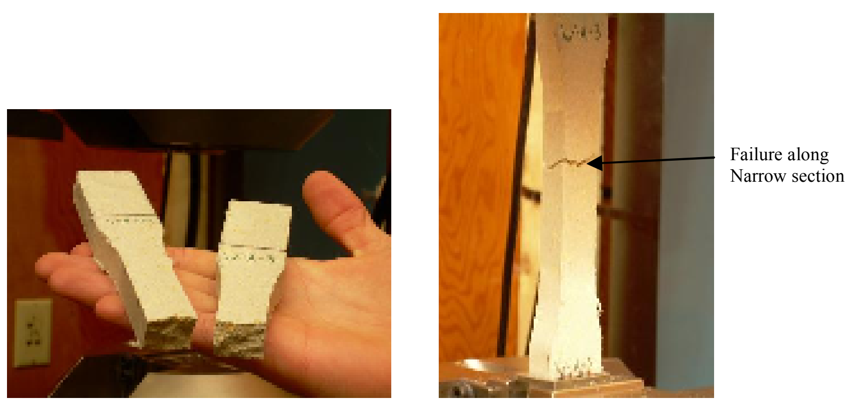

Figure 8. WPC Specimen Tension Failure.

Figure 9. Four-Point Bending Sheet piling Testing Set-up

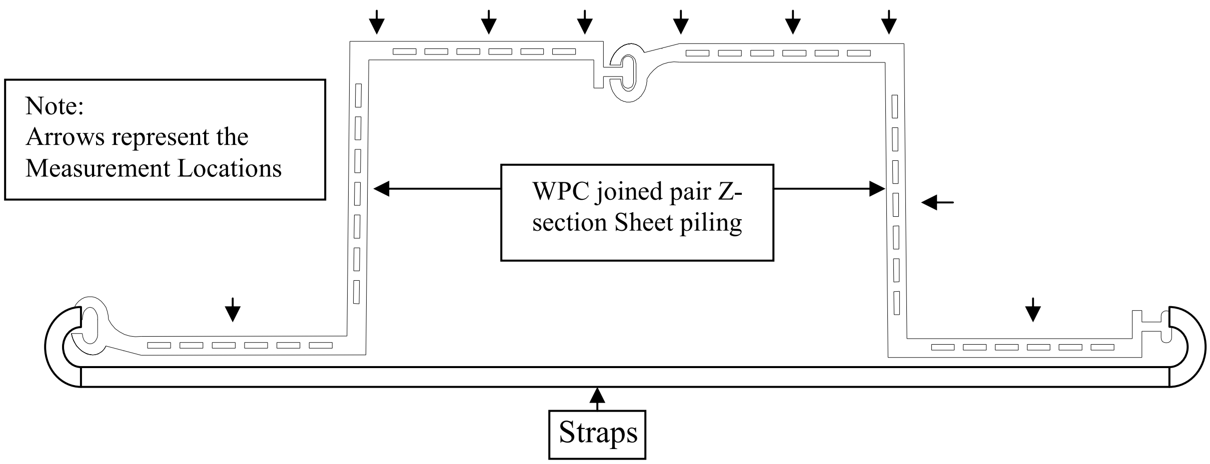

Figure 10. Deflection Measurement Locations at Mid-Span and Constrain Straps

Figure 11. Non Contact Optical 3D Measuring System. *Pontos*.

Figure 12. WPC Sheet Piling Tensile Failure.

Figure 13. WPC Sheet Piling Shear Failure.

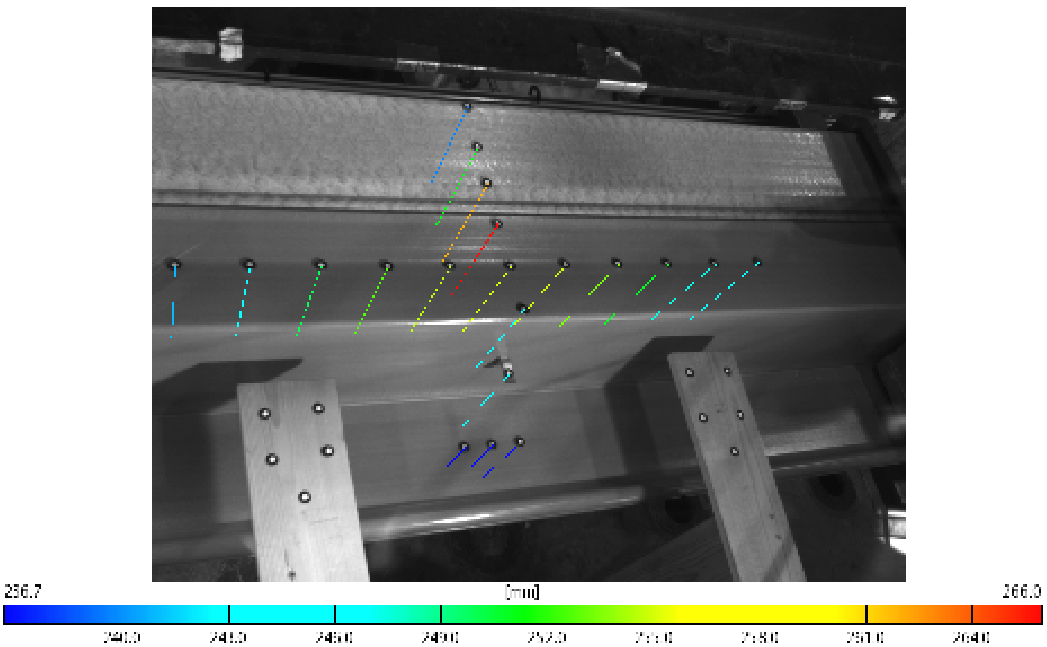

Figure 14. Four-Point Bending Displacement Field. 5.9m(19.5ft) Sheet Piling span.

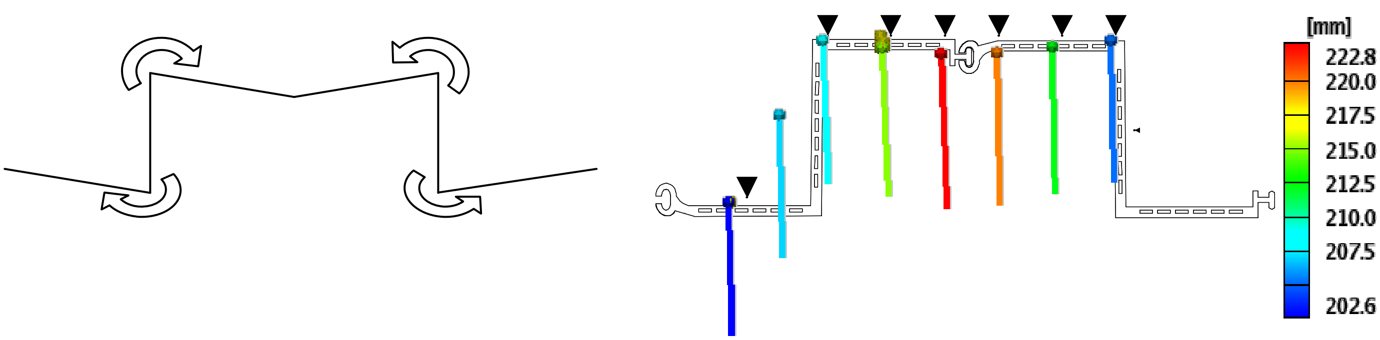

a) b)

Figure 15. Cross-Sectional Distortion during Four-Point Bending Test. a) Sketch, b) Displacement field for 5.9 m (19.5 ft) span.

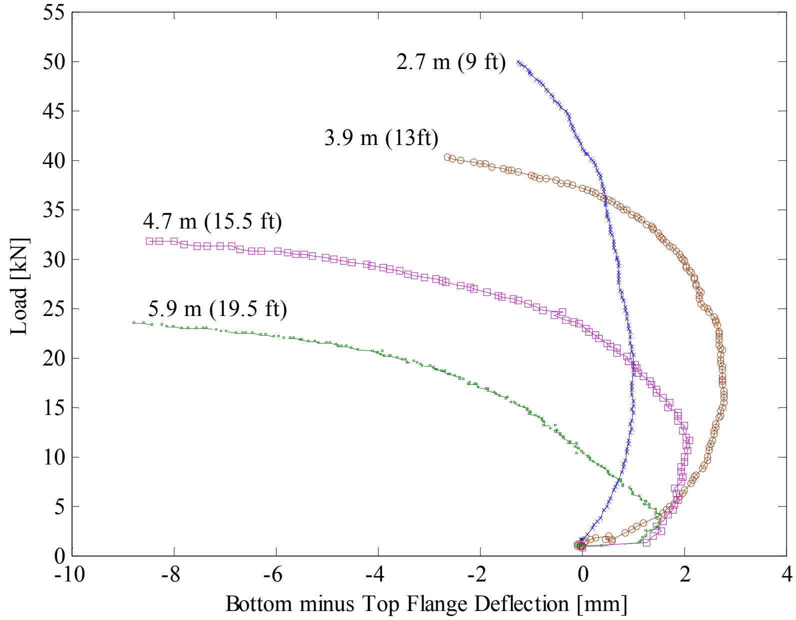

Figure 16. Typical Bottom Flange Deflection minus Top flange Deflection during Four-Point Bending Test. 1 curve per span

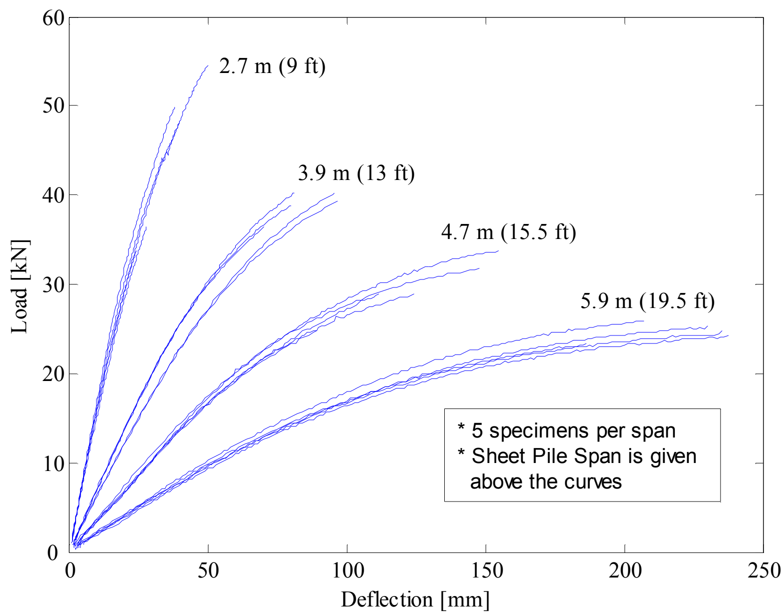

Figure 17. Load vs. Deflection Curve for WPC Sheet Pilings

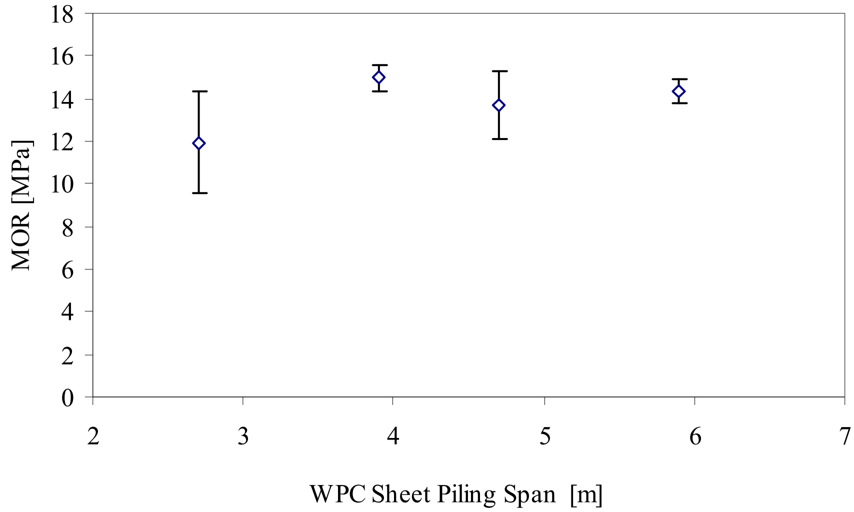

Figure 18. MOR. 5 Specimens per Span. Error Bar Represents 95% Confidence Interval for Each Span.

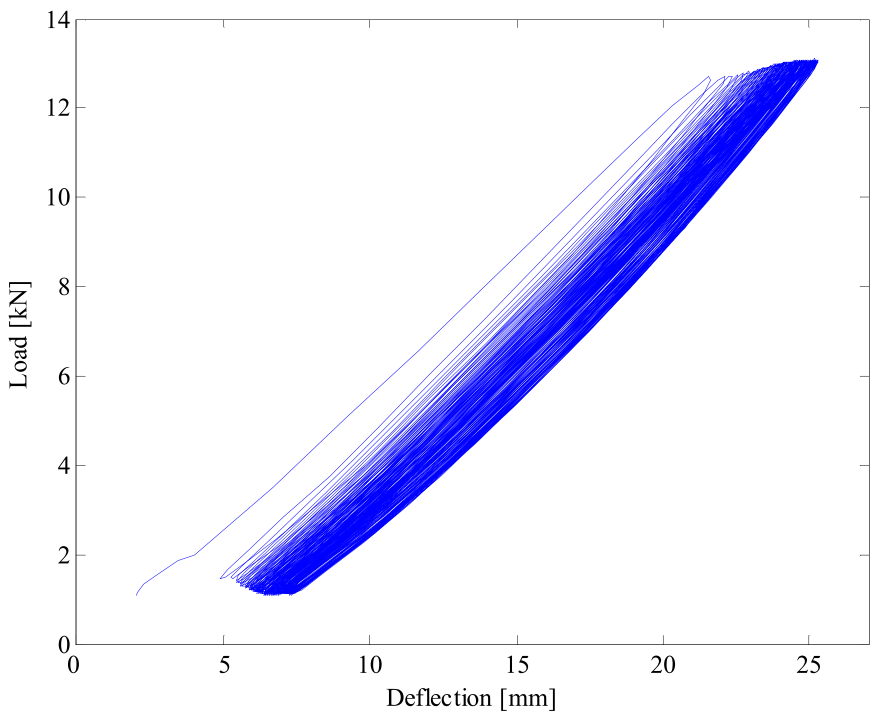

Figure 19. Load vs. Displacement Curve for Cyclic Testing at 40 % of the Mean Ultimate Strength for a WPC Sheet Piling of 3.9 m (13 ft) Span.

Tables:

Table 1. WPC Tension Test Results. 8 Specimens tested

Description	Sample Size	MOE GPa (ksi)	Ultimate Strength MPa (ksi)	Strain at Ultimate Strength (%)	Maximum Strain (%)	Strength at Maximum Strain MPa (ksi)
Mean	8	3.00 (435)	12.7 (1.84)	0.99	1.03	12.3 (1.78)
COV (%)		6	4	16	15	5

Table 2. Modulus of elasticity

Description	Source of Data	Sample Size	MOE GPa (ksi)
WPC from Sheet Piling	This paper	8 Specimens	3.00 (435)
Polypropylene	ASTM D 638	8 Laboratories	1.47 (213)
Polycarbonate	Polymer Science and Technology [16]		2.40 (348)
Polystyrene	Polymer Science and Technology [16]		2.8-3.5 (406-508)
Poly (vinyl chloride)	Polymer Science and Technology [16]		2.1-4.1 (306-595)

Note: Unit conversions based on ASTM SI 10 [17]

Table 3. WPC Four-Point Bending Test Matrix

Span m (ft)	Extreme Fiber Strain Rate (% per minute)	Sample Size Quasi-Static	Sample Size 100 Cycles followed by Quasi-Static
2.7 (9)	1	4	1
3.9 (13)	1	4	1
4.7 (15.5)	1	4	1
5.9 (19.5)	1	4	1

Table 4. WPC Sheet Piling Properties, 5 specimens per span.

Span m (ft)	Sample Size	Mean Apparent E Based on Bending Tests GPa (ksi)	COV %	Mean MOR Based on Bending Tests MPa (ksi)	COV %	Deflection at Ultimate Strength m (ft)	COV %	Failure Mode
2.7 (9)	5	5.33 (773)	5	11.9 (1.73)	20	0.036 (0.117)	29	Shear
3.9 (13)	5	6.48 (940)	7	15.0 (2.17)	4	0.082 (0.268)	15	Shear / Bending
4.7 (15.5)	5	5.91 (858)	4	13.7 (1.98)	11	0.125 (0.411)	21	Shear / Bending
5.9 (19.5)	5	6.49 (941)	3	14.3 (2.08)	4	0.219 (0.720)	10	Bending
Mean		6.05 (878)	9	13.7 (1.99)	9			

Table 5. Permanent Deformation after Cyclic Testing. 1 Specimen per Span.

Span m (ft)	Permanent deformation mm (in)	Sample Size
2.7 (9)	2 (0.07)	1
3.9 (13)	5 (0.19)	1
4.7 (15.5)	9 (0.35)	1
5.9 (19.5)	17 (0.67)	1